 

Commun. Theor. Phys. **75** (2023) 085101 (13pp) https://doi.org/10.1088/1572-9494/acdce5

# Tsallis relative $\alpha$ entropy of coherence dynamics in Grover's search algorithm

**Linlin Ye[1], Zhaoqi Wu[1,*] and Shao-Ming Fei[2]**

[1] Department of Mathematics, Nanchang University, Nanchang 330031, China
[2] School of Mathematical Sciences, Capital Normal University, Beijing 100048, China

E-mail: wuzhaoqi_conquer@163.com

Received 27 February 2023, revised 9 June 2023
Accepted for publication 9 June 2023
Published 20 July 2023

**Abstract**

Quantum coherence plays a central role in Grover's search algorithm. We study the Tsallis relative $\alpha$ entropy of coherence dynamics of the evolved state in Grover's search algorithm. We prove that the Tsallis relative $\alpha$ entropy of coherence decreases with the increase of the success probability, and derive the complementarity relations between the coherence and the success probability. We show that the operator coherence of the first $H^{\otimes n}$ relies on the size of the database $N$, the success probability and the target states. Moreover, we illustrate the relationships between coherence and entanglement of the superposition state of targets, as well as the production and deletion of coherence in Grover iterations.

Keywords: quantum coherence, Grover's search algorithm, Tsallis relative $\alpha$ entropy of coherence

(Some figures may appear in colour only in the online journal)

## 1. Introduction

Coherence is a fundamental property of quantum mechanics that stems from the quantum superposition principle. Quantification of coherence is one of the most important problems in the study of quantum coherence. Baumgratz, Gramer and Plenio [1] constituted a rigorous framework to quantify coherence from the viewpoint of quantum resource theories [2, 3] which is powerful and highly versatile. Based on this framework, some coherence measures have been proposed [4–7]. An alternative framework for quantifying coherence [8] has been formulated, and some other coherence measures [9, 10] have been presented. These frameworks stimulated further research on relationships with other quantum resources [11–14], coherence dynamics and related problems [15–27], and coherence quantification in infinite-dimensional systems [28, 29]. As a significant physical resource, coherence has diverse applications in biological systems [30, 31], thermodynamical systems [32–36], nanoscale physics [37], and quantum phase transition [38].

Quantum algorithms may be able to solve problems that are classically difficult. The factorization of large integers is considered to be a notoriously difficult problem on a classical device. There is no classical factorization algorithm with polynomial run-time. Shor's quantum factorization algorithm [39] gives a superpolynomial speedup over all known classical factorization algorithms [40, 41]. Hassidim and Lloyd [42] proposed the Harrow–Hassidim–Lloyd (HHL) algorithm for solving linear systems of equations and proved that any classical algorithm generically requires exponentially more time than the HHL algorithm.

The well-known Grover's search algorithm (GSA) has been widely used in quantum information processing, which provides a quadratic temporal speedup over classical search algorithms. It has been pointed out that GSA is the repetition of the application of Grover operator $G$ [43], which can be decomposed into $G = H^{\otimes n}PH^{\otimes n}O$, where $H$, $P$ and $O$ are Hadamard operator, condition phase-shift operator and oracle operator, respectively. The great utility of the algorithm arises from the fact that one does not need to assume any particular structures of the database. As a crucial resource, entanglement plays a significant role [44–46] in GSA. Pan, Qiu, Mateus and Gruska [47] have shown that the oracle operator $O$ and the reflection operator $R$ contribute to entanglement in GSA, and demonstrated that there exists a turning point during Grover's iteration application.

* Author to whom any correspondence should be addressed.

Tsallis entropy [48] is an extension of Shannon entropy, which plays an important role in nonextensive statistics. Tsallis relative entropy offers an information-theoretic basis for measuring the difference between two given distributions and establishes a convergence property. Its applications in the classical system has been studied in [49–51]. Quantum Tsallis relative $\alpha$ entropy [52, 53] is a superior information-theoretic measure of the degree of state purification compared with classical case, and it is monotonic under trace preserving completely positive linear map without the requirement that density operators are invertible [54]. A quantum coherence quantifier based on Tsallis relative $\alpha$ entropy has been first proposed in [55], which satisfies the monotonicity and variational monotonicity, but not the strong monotonicity. Zhao and Yu [56] proposed a modified well-defined quantifier for which the strong monotonicity holds. For Tsallis relative $\alpha$ entropy, the required minimization can be solved with an explicit answer.

Noteworthily, Tsallis relative $\alpha$ entropy of coherence reduces to the standard relative entropy of coherence when $\alpha \to 1$, and reduces to the skew information of coherence when $\alpha = \frac{1}{2}$, up to a constant factor. The relative entropy of coherence can be understood as the optimal rate for distilling a maximally coherent state from given states [2] and has a close connection with entanglement [57]. The tradeoff relation of relative entropy of coherence not only depends on the state but is also accompanied by the basis-free coherence [23]. The skew information of coherence has an obvious operational meaning based on quantum metrology, and forms the natural upper bounds for quantum correlations prepared by incoherent operations [6]. It characterizes the contribution of the commutation between the density matrix of interest and the broken observable. The skew information and $l_1$ norm can induce the experimentally measurable bounds of coherence, while the relative entropy of coherence can be exactly measured in experiment in principle. Interestingly, Tsallis relative $\alpha$ entropy of coherence and $l_1$ norm of coherence give the same ordering for single-qubit pure states [58].

The role of coherence in quantum algorithms has attracted considerable attention in recent years [59–66]. It has been found that the Deutsch–Jozsa algorithm relies on coherence during the processing, and its precision is directly related to the recoverable coherence [67, 68]. Following their footsteps, Pan and Qiu [69] have explored the coherence dynamics of each basic operator in GSA, and the coherence production and depletion in terms of the $l_1$ norm of coherence. Likewise, similar methods have been applied to other algorithms, including the Deutsch–Jozsa algorithm and Shor's algorithm [70], and it is found that coherence depletion always exists [70, 71]. Pan, Situ and Zheng [72] have displayed the complementarity relation between coherence and the success probability in GSA via the $l_1$ norm of coherence. Coherence determines the performance of Shor's algorithm by bounding the success probability from below and above [73]. Decoherence in quantum algorithms has been studied [74–78], and coherence has been explored alongside entanglement in algorithms [74, 79–81]. The role of coherence playing in the deterministic quantum computation with one qubit model has been investigated explicitly [82–86].

In this paper, we study the coherence dynamics and derive the complementarity relations between the success probability and coherence in GSA based on Tsallis relative $\alpha$ entropy. The rest of the paper is organized as follows. In section 2, we recall GSA and Tsallis relative $\alpha$ entropy of coherence, study the dynamics of the Tsallis relative $\alpha$ entropy of coherence in GSA, and explore the complementarity relations between coherence and the success probability. In section 3, we investigate the coherence dynamics of the state after each basic operator is applied in GSA. In section 4, we study the Tsallis relative $\alpha$ entropy of coherence dynamics for different cases of the target states. By identifying the variations before and after the basic operators are imposed, we explore the coherence depletion and production in section 5. In section 6, we compare our work with previous works on coherence dynamics in GSA. Finally, we summarize our results and discuss further problems in section 7.

## 2. Tsallis relative $\alpha$ entropy of coherence in GSA and complementarity relations

In section 2.1, we first review the concepts of the Tsallis relative $\alpha$ entropy of coherence and GSA, and then study the coherence dynamics in GSA. We investigate the complementarity relations between coherence and success probability in section 2.2.

### 2.1. Tsallis relative $\alpha$ entropy of coherence in GSA

The Tsallis relative $\alpha$ entropy is defined by [52, 53]

$$D_\alpha(\rho\|\sigma) = \frac{1}{\alpha - 1}(f_\alpha(\rho, \sigma) - 1),\ \alpha \in (0,1) \bigcup (1,\infty), \tag{1}$$

where

$$f_\alpha(\rho, \sigma) = \mathrm{Tr}(\rho^\alpha \sigma^{1-\alpha}).$$

It is shown that when $\alpha \to 1$, $D_\alpha(\rho\|\sigma)$ reduces to $S'(\rho\|\sigma) = \ln 2 S(\rho\|\sigma)$, where $S(\rho\|\sigma) = \mathrm{Tr}(\rho \log \rho) - \mathrm{Tr}(\rho \log \sigma)$ is the standard relative entropy between two quantum states $\rho$ and $\sigma$, and the logarithm 'log' is taken to be base 2. With respect to a fixed orthonormal basis $\{|j\rangle\}_{j=1}^d$ in a $d$ dimensional Hilbert space, based on Tsallis relative $\alpha$ entropy the coherence $\tilde{C}_\alpha(\rho)$ of a density operator $\rho$ is defined by [55]

$$\begin{aligned}\tilde{C}_\alpha(\rho) &= \min_{\sigma\in\mathcal{I}} D_\alpha(\rho\|\sigma) \\ &= \frac{1}{\alpha - 1}\left[\left(\sum_{j=1}^d \langle j|\ \rho^\alpha\ |j\rangle^{\frac{1}{\alpha}}\right)^\alpha - 1\right],\end{aligned} \tag{2}$$

where $\mathcal{I}$ denotes the set of incoherent states. It is worthwhile to note that $\tilde{C}_\alpha(\rho)$ does not satisfy the strong monotonicity [55], and thus $\tilde{C}_\alpha(\rho)$ is not a good coherence measure. A

well-defined coherence quantifier based on Tsallis relative $\alpha$ entropy has been presented for $\alpha \in (0,1) \cup (1,2]$ [56],

$$C_\alpha(\rho) = \min_{\sigma\in\mathcal{I}} \frac{1}{\alpha-1}(f_\alpha^{\frac{1}{\alpha}}(\rho,\sigma)-1) = \frac{1}{\alpha-1}\left[\sum_{j=1}^{d}\langle j|\ \rho^\alpha\ |j\rangle^{\frac{1}{\alpha}} - 1\right]. \tag{3}$$

$C_\alpha(\rho)$ reduces to $\ln 2C_r(\rho)$ when $\alpha \to 1$, where $C_r(\rho) = \mathrm{Tr}(\rho\log\rho) - \mathrm{Tr}(\rho_{\mathrm{diag}}\log\rho_{\mathrm{diag}})$ is the relative entropy of coherence [1]. When $\alpha = \frac{1}{2}$, $C_\alpha(\rho)$ reduces to $2C_s(\rho)$, where $C_s(\rho)=1-\sum_{j=1}^{d}\langle j|\ \sqrt{\rho}\ |j\rangle^2$ is the skew information of coherence [6].

Let $N=2^n$ be the number of elements of the database, and $t$ the amount of target states that meet some specific conditions in the database. The purpose of the search algorithm is to seek out the target states from the database. GSA makes use of a single $n$ qubit register, starts with an $n$-qubit pure state $|0\rangle^{\otimes n}$ and applies the Hadamard operator $H$ to get an equal superposed state,

$$|\psi\rangle = \frac{1}{\sqrt{N}}\sum_{x=0}^{N-1}|x\rangle.$$

It is useful to adopt the convention that $|\chi_0\rangle$ denotes the sum of all not-target states $|x_n\rangle$, and $|\chi_1\rangle$ the sum of all target states $|x_s\rangle$,

$$|\chi_0\rangle = \frac{1}{\sqrt{N-t}}\sum_{x_n}|x_n\rangle,\ |\chi_1\rangle = \frac{1}{\sqrt{t}}\sum_{x_s}|x_s\rangle.$$

Simple algebra shows that $|\psi\rangle$ can be expressed as

$$|\psi\rangle = \sqrt{\frac{N-t}{N}}|\chi_0\rangle + \sqrt{\frac{t}{N}}|\chi_1\rangle. \tag{4}$$

The quantum algorithm repeats the application of a quantum subroutine $G = H^{\otimes n}PH^{\otimes n}O$ named as the Grover iteration or Grover operator. $G$ can be decomposed into four steps:

(i) Apply the oracle operator $O = I - 2\sum_{x_s}|x_s\rangle\langle x_s| = \sum_x(-1)^{f(x)}|x\rangle\langle x|$.

(ii) Apply the Hadamard transform $H^{\otimes n} = \frac{1}{\sqrt{N}}\sum_{x,y}(-1)^{xy}\times|y\rangle\langle x|$.

(iii) Perform a conditional phase shift operator $P = 2|0\rangle\langle 0| - I = \sum_x -(-1)^{\delta_{x0}}|x\rangle\langle x|$.

(iv) Apply the Hadamard transform $H^{\otimes n}$.

Set $\sin\theta = \sqrt{\frac{t}{N}}$ and $\cos\theta = \sqrt{\frac{N-t}{N}}$. We have $|\psi\rangle = \cos\theta|\chi_0\rangle + \sin\theta|\chi_1\rangle$. After $k$ iterations of the Grover operator, the state $|\psi\rangle$ transforms into $|\psi_k\rangle = \cos\theta_k|\chi_0\rangle + \sin\theta_k|\chi_1\rangle$, where $\theta_k = (2k+1)\theta$. Conventionally, denote $A_k = \cos\theta_k$ and $B_k = \sin\theta_k$. One has

$$|\psi_k\rangle = A_k|\chi_0\rangle + B_k|\chi_1\rangle. \tag{5}$$

Let $\rho_k = |\psi_k\rangle\langle\psi_k|$ be the density operator of the state $|\psi_k\rangle$. The success probability can be expressed as $P_k = \sin^2\theta_k$. Combining equation (3) with (5), we have

$$C_\alpha(\rho_k) = \frac{1}{\alpha-1}[(1-P_k)^{\frac{1}{\alpha}}(N-t)^{1-\frac{1}{\alpha}} + P_k^{\frac{1}{\alpha}}t^{1-\frac{1}{\alpha}} - 1]. \tag{6}$$

Under the condition $t \ll N$, we have from equation (6)

- when $\alpha \in (0, 1)$,

$$C_\alpha(\rho_k) \simeq \frac{1}{\alpha-1}(P_k^{\frac{1}{\alpha}}t^{1-\frac{1}{\alpha}} - 1), \tag{7}$$

- when $\alpha \in (1, 2]$,

$$C_\alpha(\rho_k) \simeq \frac{N}{\alpha-1}\left(\frac{1-P_k}{N}\right)^{\frac{1}{\alpha}}. \tag{8}$$

**Remark 2.1.** Set $\alpha = \frac{1}{2}$ in equation (7). The skew information of coherence of the state $|\psi_k\rangle$ is given by

$$C_s(\rho_k) \simeq 1 - \frac{P_k^2}{t}. \tag{9}$$

Under the limit $\alpha \to 1$, from equation (6) the relative entropy of coherence of the state $|\psi_k\rangle$ is

$$\begin{aligned} C_r(\rho_k) &= \tfrac{1-P_k}{\ln 2}\ln\tfrac{N-t}{1-P_k} + \tfrac{P_k}{\ln 2}\ln\tfrac{t}{P_k} \\ &\simeq \tfrac{1-P_k}{\ln 2}\ln\tfrac{N}{1-P_k}. \end{aligned} \tag{10}$$

Here $A \simeq B$ means that $A$ asymptotically equals to $B$ under the condition $t \ll N$. When the success probability is increasing, according to equations (7) and (8), we obtain that the coherence is decreasing, i.e. coherence decreases with the increase of the success probability. In particular, from equation (6), when the success probability reaches 1, the coherence is $C_\alpha(\rho_k) = \frac{1}{\alpha-1}(t^{1-\frac{1}{\alpha}} - 1)$. In other words, the success probability relies on the coherence depletion in terms of Tsallis relative $\alpha$ entropy of coherence.

### *2.2. Complementarity relations between Tsallis relative $\alpha$ entropy of coherence and success probability*

For a qubit state $|\phi\rangle = \cos\frac{\theta}{2}|0\rangle + e^{i\varphi}\sin\frac{\theta}{2}|1\rangle$, the density matrix $\rho = |\phi\rangle\langle\phi|$ has the form,

$$\rho = \frac{1}{2}\begin{pmatrix} 1+r_z & r_x - ir_y \\ r_x + ir_y & 1-r_z \end{pmatrix},$$

with the Bloch vector $\boldsymbol{r} = (r_x, r_y, r_z) = (\sin\theta\cos\varphi, \sin\theta\times\sin\varphi, \cos\theta)$. The Bloch vector of the original state $|\psi\rangle = \cos\theta|\chi_0\rangle + \sin\theta|\chi_1\rangle$ in GSA is $\boldsymbol{r}(0) = (\sin 2\theta, 0, \cos 2\theta)$. Since $r_y = 0$, the Grover iteration $G$ in the Bloch representation is given by

$$G = \begin{bmatrix} \cos 2\theta & -\sin 2\theta \\ \sin 2\theta & \cos 2\theta \end{bmatrix}.$$

After $k$ iterations, we have

$$G^k = \begin{bmatrix} \cos 2\theta_k & -\sin 2\theta_k \\ \sin 2\theta_k & \cos 2\theta_k \end{bmatrix}.$$

From

$$\begin{bmatrix} r_x(k) \\ r_z(k) \end{bmatrix} = G^k \begin{bmatrix} r_x(0) \\ r_z(0) \end{bmatrix} = G^k \begin{bmatrix} \sin 2\theta \\ \cos 2\theta \end{bmatrix},$$

we obtain $r_x(k) \simeq -\sin 2\theta_k$ and $r_z(k) \simeq \cos 2\theta_k$ when $t \ll N$.

Following the idea in [72], we define the normalized $C_\alpha$ as

$$N(C_\alpha) = C_\alpha / C_\alpha^{\max}. \tag{11}$$

Obviously, $N(C_\alpha) \in [0,\ 1]$.

**Theorem 1.** The Tsallis relative $\alpha$ entropy of coherence and the success probability satisfies the following complementary relations in GSA for $t \ll N$.

(1) For $\alpha \in (0,1)$, it holds that

$$N(C_\alpha) + P_k^{\frac{1}{\alpha}} t^{1-\frac{1}{\alpha}} \simeq 1. \tag{12}$$

(2) For $\alpha \in (1,2]$, it holds that

$$[N(C_\alpha)]^\alpha + P_k \simeq 1, \tag{13}$$

where $\simeq$ means the algorithm search in a large database satisfying $t \ll N$.

*Proof*. Since $r_x(k) \simeq -\sin 2\theta_k$ and $r_z(k) \simeq \cos 2\theta_k$, simple calculation yields that $\cos^2\theta_k \simeq \frac{1}{2}(1 + r_z(k))$ and $\sin^2\theta_k \simeq \frac{1}{2}(1 - r_z(k))$. According to equation (6), we have

$$C_\alpha(\rho_k) = \frac{1}{\alpha - 1}[(\cos^2\theta_k)^{\frac{1}{\alpha}}(N-t)^{1-\frac{1}{\alpha}} + (\sin^2\theta_k)^{\frac{1}{\alpha}} t^{1-\frac{1}{\alpha}} - 1].$$

When $\alpha \in (0,\ 1)$, $t \ll N$, we obtain

$$C_\alpha(\rho_k) \simeq \frac{1}{1-\alpha}\left[1 - \left(\frac{1 - r_z(k)}{2t}\right)^{\frac{1}{\alpha}} t\right]. \tag{14}$$

Since $r_z(k) \in [0,\ 1]$, the maximum of $C_\alpha$ is

$$C_\alpha^{\max} \simeq \frac{1}{1-\alpha}. \tag{15}$$

Then we have

$$N(C_\alpha) \simeq 1 - \left(\frac{1 - r_z(k)}{2t}\right)^{\frac{1}{\alpha}} t. \tag{16}$$

Since $P_k = \sin^2\theta_k \simeq \frac{1}{2}(1 - r_z(k))$, when $t \ll N$ and $\alpha \in (0,\ 1)$, we get the complementarity relation (12).

When $\alpha \in (1,\ 2]$, $t \ll N$, we obtain

$$C_\alpha(\rho_k) \simeq \frac{N}{\alpha - 1}\left(\frac{1 + r_z(k)}{2N}\right)^{\frac{1}{\alpha}}. \tag{17}$$

Since $r_z(k) \in [0,\ 1]$, we have

$$C_\alpha^{\max} \simeq \frac{N}{\alpha - 1}\left(\frac{1}{N}\right)^{\frac{1}{\alpha}}, \tag{18}$$

and

$$[N(C_\alpha)]^\alpha \simeq \frac{1 + r_z(k)}{2}. \tag{19}$$

As $P_k = \sin^2\theta_k \simeq \frac{1}{2}(1 - r_z(k))$, when $t \ll N$ and $\alpha \in (1, 2]$, we get the complementarity relation (13) between coherence and success probability. This completes the proof. □

**Remark 2.2.** When $\alpha = \frac{1}{2}$ in equation (12), the complementarity relation between skew information of coherence and success probability is of the form,

$$N(C_s) + \frac{1}{t}P_k^2 \simeq 1.$$

At the limit $\alpha \to 1$, equation (6) gives rise to

$$C_r(\rho_k) \simeq \frac{1 + r_z}{2\ln 2} \ln \frac{2N}{1 + r_z}.$$

When $r_z = 1$, we have

$$C_r^{\max} \simeq \frac{1}{\ln 2}\ln N,\ N(C_r) \simeq \frac{1 + r_z}{2}.$$

Since $P_k = \sin^2\theta_k \simeq \frac{1}{2}(1 - r_z(k))$, we obtain the complementarity relation between relative entropy of coherence and success probability, $N(C_r) + P_k \simeq 1$.

According to equations (12) and (13), when $\alpha \in (0,\ 1)$ and $P_k = 1$, normalization of coherence satisfies $N(C_\alpha) + t^{1-\frac{1}{\alpha}} \simeq 1$. When $\alpha \in (1,\ 2]$ and $P_k = 1$, normalization of coherence satisfies $N(C_\alpha) \simeq 0$. Noting that $N(C_\alpha)$ is the normalization of $C_\alpha$, and $A \simeq B$ means that $A$ is asymptotically equal to $B$ under the condition $t \ll N$, this does not necessarily mean that $C_\alpha$ is asymptotically equal to 0, let alone it is equal to 0.

## 3. Dynamics of the Tsallis relative $\alpha$ entropy of coherence in GSA

In this section, we investigate the coherence of the state after each basic operator is applied in the Grover iteration.

Denote the first $H^{\otimes n}$ and the second $H^{\otimes n}$ by $H_O$ and $H_P$, respectively. In [21,87] it has been shown that $U = \sum_i e^{j\alpha_i}|\beta(i)\rangle\langle i|$ is the general form of any of the unitary incoherent operators, where $\beta(i)$ is relabeling of $\{i\}$. Hence, the oracle operator $O$ and the condition phase-shift operator $P$ are incoherent operators. Moreover, both $O$ and $P$ do not change the coherence. Denote $|\psi_{kO}\rangle$ the state after $O$ is applied on $|\psi_k\rangle$ and $\rho_{kO} = |\psi_{kO}\rangle\langle\psi_{kO}|$. We have

$$|\psi_{kO}\rangle \equiv O|\psi_k\rangle = A_k|\chi_0\rangle - B_k|\chi_1\rangle. \tag{20}$$

Combining equation (3) with (5), we have $C_\alpha(\rho_{kO}) = C_\alpha(\rho_k)$, where $\alpha \in (0,\ 1) \cup (1,\ 2]$.

In the computational basis, the $N$-dimensional Hadamard matrix has the following three properties: (i) The common coefficient is $\frac{1}{\sqrt{N}}$. (ii) The elements of the first row and the first column are 1. (iii) In any other rows or columns, a half of the elements are 1, and the others are $-1$. Let $H_{y,x}$ denote the element of the $y$th row and the $x$th column in a Hadamard matrix and $t_y$ denote the number of $H_{y,x} = 1$, $t_y = |\{H_{y,x}|H_{y,x} = 1,\ x \in \{x_s\}\}|$. Denote by $|\psi_{kH_O}\rangle$ the state

after $H_O$ is applied on $|\psi_{kO}\rangle$ and $|\psi_{kH_P}\rangle$ the state after $H_P$ is applied on $PH^{\otimes n}|\psi_{kO}\rangle$. We have

$$\begin{aligned}|\psi_{kH_O}\rangle &\equiv H^{\otimes n}|\psi_{kO}\rangle \\ &= \left[\frac{1}{\sqrt{N}}\sum_{y=0}^{N-1}\frac{A_k}{\sqrt{N-t}}\sum_{x\in\{x_n\}}(-1)^{xy}\right. \\ &\left. -\frac{1}{\sqrt{N}}\sum_{y=0}^{N-1}\frac{B_k}{\sqrt{t}}\sum_{x\in\{x_s\}}(-1)^{xy}\right]|y\rangle, \end{aligned} \tag{21}$$

and

$$|\psi_{kH_P}\rangle \equiv H^{\otimes n}PH^{\otimes n}|\psi_{kO}\rangle = |\psi_{k+1}\rangle. \tag{22}$$

**Theorem 2.** The Tsallis relative $\alpha$ entropy of coherence of the states $|\psi_{kH_O}\rangle$ and $|\psi_{kH_P}\rangle$ are given by

$$C_\alpha(\rho_{kH_O}) \simeq \frac{1}{\alpha-1}[(P_k\gamma(t,t_y))^{\frac{1}{\alpha}}N^{1-\frac{1}{\alpha}}-1], \tag{23}$$

and

$$C_\alpha(\rho_{kH_P}) \simeq \frac{1}{\alpha-1}(P_{k+1}^{\frac{1}{\alpha}}t^{1-\frac{1}{\alpha}}-1), \tag{24}$$

respectively for $t \ll N$ and $\alpha \in (0,\ 1)$, and

$$C_\alpha(\rho_{kH_O}) \simeq \frac{N}{\alpha-1}\left(\frac{P_k\gamma(t,t_y)}{N}\right)^{\frac{1}{\alpha}}, \tag{25}$$

and

$$C_\alpha(\rho_{kH_P}) \simeq \frac{N}{\alpha-1}\left(\frac{1-P_{k+1}}{N}\right)^{\frac{1}{\alpha}}, \tag{26}$$

respectively for $t \ll N$ and $\alpha \in (1,\ 2]$, where $\gamma(t,t_y) = \frac{(t-2t_y)^2}{t}$ and $P_k = \sin^2\theta_k$.

*Proof*. From equation (21) $|\psi_{kH_O}\rangle$ can be reexpressed as

$$\begin{aligned}|\psi_{kH_O}\rangle &= \frac{1}{\sqrt{N}}[(A_k\sqrt{N-t}-B_k\sqrt{t})|0\rangle \\ &\left.+\sum_{y\neq 0}(t-2t_y)\left(\frac{A_k}{\sqrt{N-t}}+\frac{B_k}{\sqrt{t}}\right)|y\rangle\right]. \end{aligned} \tag{27}$$

According to equation (22), we obtain

$$|\psi_{kH_P}\rangle \equiv H^{\otimes n}PH^{\otimes n}|\psi_{kO}\rangle = |\psi_{k+1}\rangle = A_{k+1}|\chi_0\rangle + B_{k+1}|\chi_1\rangle. \tag{28}$$

By straightforward derivation we have

$$\begin{aligned}\rho_{kH_O} &= |\psi_{kH_O}\rangle\langle\psi_{kH_O}| \\ &= \frac{1}{N}\left[(A_k\sqrt{N-t}-B_k\sqrt{t})^2|0\rangle\langle 0| + \sum_{y\neq 0}(t-2t_y)\right. \\ &\times\left(\frac{A_k}{\sqrt{N-t}}+\frac{B_k}{\sqrt{t}}\right)(A_k\sqrt{N-t}-B_k\sqrt{t})(|0\rangle\langle y| + |y\rangle\langle 0|) \\ &\left.+\sum_{y,\,y'\neq 0}(t-2t_y)(t-2t_{y'})\left(\frac{A_k}{\sqrt{N-t}}+\frac{B_k}{\sqrt{t}}\right)^2|y\rangle\langle y'|\right], \end{aligned} \tag{29}$$

and $\rho_{kH_P} = |\psi_{kH_P}\rangle\langle\psi_{kH_P}| = \rho_{k+1}$.

Combining equation (3) with (29) we have

$$\begin{aligned}C_\alpha(\rho_{kH_O}) = \frac{1}{\alpha-1}\left[\frac{(A_k\sqrt{N-t}-B_k\sqrt{t})^{\frac{2}{\alpha}}}{N^{\frac{1}{\alpha}}}\right. \\ \left.+(N-1)\frac{(t-2t_y)^{\frac{2}{\alpha}}\left(\frac{A_k}{\sqrt{N-t}}+\frac{B_k}{\sqrt{t}}\right)^{\frac{2}{\alpha}}}{N^{\frac{1}{\alpha}}}-1\right]. \end{aligned} \tag{30}$$

Since $\rho_{kH_P} = \rho_{k+1}$, we have $C_\alpha(\rho_{kH_P}) = C_\alpha(\rho_{k+1})$ and

$$\begin{aligned}&C_\alpha(\rho_{kH_P}) \\ &= \frac{1}{\alpha-1}[(1-P_{k+1})^{\frac{1}{\alpha}}(N-t)^{1-\frac{1}{\alpha}} + P_{k+1}^{\frac{1}{\alpha}}t^{1-\frac{1}{\alpha}}-1]. \end{aligned} \tag{31}$$

Denote $\gamma(t,t_y) = \frac{(t-2t_y)^2}{t}$. Noting that $t \ll N$, when $\alpha \in (0,\ 1)$ we have (23) and (24), and we have (25) and (26) when $\alpha \in (1,\ 2]$. □

**Remark 3.1.** Set $\alpha = \frac{1}{2}$ in equations (23) and (24). The skew information of coherence of the states $|\psi_{kH_O}\rangle$ and $|\psi_{kH_P}\rangle$ satisfy

$$C_s(\rho_{kH_O}) \simeq 1 - \frac{(\gamma(t,t_y)P_k)^2}{N} \text{ and } C_s(\rho_{kH_P}) \simeq 1 - \frac{P_{k+1}^2}{t}, \tag{32}$$

respectively. When $\alpha \to 1$ in equation (30), according to equation (10), the relative entropies of coherence of the state $|\psi_{kH_O}\rangle$ and $|\psi_{kH_P}\rangle$ satisfy

$$\begin{aligned}C_r(\rho_{kH_O}) &\simeq \frac{\gamma(t,t_y)P_k}{\ln 2}\ln\frac{N}{\gamma(t,t_y)P_k} \\ \text{and } C_r(\rho_{kH_P}) &\simeq \frac{1-P_{k+1}}{\ln 2}\ln\frac{N}{1-P_{k+1}}, \end{aligned} \tag{33}$$

respectively. Based on Theorem 2, it is easy to see that the coherence of the state $|\psi_{kH_O}\rangle$ is related to the size of the database $N$, success probability $P_k$ and target states. The coherence of the state $|\psi_{kH_P}\rangle$ is dependent on $N$ and $P_k$.

## 4. Different target states

In this section, we discuss the coherence of the state $|\psi_{kH_O}\rangle$ for special target states, i.e. the superposition state $|\chi_1\rangle$ is a product state, and the target numbers are $t \leqslant 4$. We have the following result.

**Theorem 3** Suppose that the superposition state $|\chi_1\rangle$ is a product state. Then when $t \ll N$ the Tsallis relative $\alpha$ entropy of coherence of the state $|\psi_{kH_O}\rangle$ is given by

$$C_\alpha(\rho_{kH_O}) \simeq \frac{1}{\alpha-1}\left[\left(\frac{P_k}{t}\right)^{\frac{1}{\alpha}}N^{1-\frac{1}{\alpha}}-1\right], \tag{34}$$

for $\alpha \in (0,\ 1)$, and

$$C_\alpha(\rho_{kH_O}) \simeq \frac{N}{\alpha-1}\left(\frac{P_k}{Nt}\right)^{\frac{1}{\alpha}}, \tag{35}$$

for $\alpha \in (1,2]$.

*Proof*. Denote $|\chi_{0H}\rangle = H^{\otimes n}|\chi_0\rangle$ and $|\chi_{1H}\rangle = H^{\otimes n}|\chi_1\rangle$. Since $|\chi_1\rangle = \frac{1}{\sqrt{t}}\sum_{x_s}|x_s\rangle$ is the product of $n$ single-qubit states of the forms either $|0\rangle, |1\rangle$ or $(|0\rangle \pm |1\rangle)/\sqrt{2}$, $|\psi_{kH_O}\rangle$ can be written as

$$\begin{aligned}|\psi_{kH_O}\rangle &= H^{\otimes n}(A_k|\chi_0\rangle - B_k|\chi_1\rangle)\\ &= H^{\otimes n}A_k|\chi_0\rangle - H^{\otimes n}B_k|\chi_1\rangle\\ &= A_k|\chi_{0H}\rangle - B_k|\chi_{1H}\rangle,\end{aligned} \tag{36}$$

and

$$\begin{aligned}\rho_{kH_O} = A_k^2|\chi_{0H}\rangle\langle\chi_{0H}| - A_kB_k(|\chi_{1H}\rangle\langle\chi_{0H}|\\ + |\chi_{0H}\rangle\langle\chi_{1H}|) + B_k^2|\chi_{1H}\rangle\langle\chi_{1H}|,\end{aligned} \tag{37}$$

where

$$|\chi_{0H}\rangle = \sum_{y=0}^{N-1}\sum_{x\in\{x_n\}}(-1)^{xy}\frac{1}{\sqrt{N(N-t)}}|y\rangle,$$

and

$$|\chi_{1H}\rangle = \sum_{y=0}^{N-1}\sum_{x\in\{x_s\}}(-1)^{xy}\frac{1}{\sqrt{Nt}}|y\rangle.$$

After a simple transformation, we have

$$|\chi_{0H}\rangle = \sqrt{\frac{N-t}{N}}|0\rangle + \sum_{y\neq 0}\frac{t-2t_y}{\sqrt{N(N-t)}}|y\rangle, \tag{38}$$

and

$$|\chi_{1H}\rangle = \sqrt{\frac{t}{N}}|0\rangle + \sum_{y\neq 0}\frac{2t_y-t}{\sqrt{Nt}}|y\rangle. \tag{39}$$

Consequently, we derive that

$$\begin{aligned}C_\alpha(\rho_{kH_O}) = \frac{1}{\alpha-1}\Bigg[\left(\frac{A_k^2(N-t)}{N} - 2A_kB_k\sqrt{\frac{(N-t)t}{N^2}} + \frac{B_k^2t}{N}\right)^{\frac{1}{\alpha}}\\ + (N-1)\left(A_k^2\frac{(t-2t_y)^2}{N(N-t)} - 2A_kB_k\frac{(t-2t_y)(2t_y-t)}{N\sqrt{(N-t)t}} + B_k^2\frac{(2t_y-t)^2}{Nt}\right)^{\frac{1}{\alpha}} - 1\Bigg].\end{aligned} \tag{40}$$

When $t \ll N$, $\alpha \in (0,\ 1)$, and $P_k = \sin^2\theta_k$, we have

$$\begin{aligned}&C_\alpha(\rho_{kH_O})\\ &\simeq \frac{1}{\alpha-1}\left[\left(\frac{B_k^2t}{N}\right)^{\frac{1}{\alpha}} + (N-1)\left(B_k^2\frac{(2t_y-t)^2}{Nt}\right)^{\frac{1}{\alpha}} - 1\right]\\ &\simeq \frac{1}{\alpha-1}\left[\left(\frac{P_k}{t}\right)^{\frac{1}{\alpha}}N^{1-\frac{1}{\alpha}} - 1\right],\end{aligned} \tag{41}$$

and when $t \ll N$, $\alpha \in (1, 2]$, $C_\alpha(\rho_{kH_O})$ takes the form

$$\begin{aligned}&C_\alpha(\rho_{kH_O})\\ &\simeq \frac{1}{\alpha-1}\left[\left(\frac{B_k^2t}{N}\right)^{\frac{1}{\alpha}} + (N-1)\left(B_k^2\frac{(2t_y-t)^2}{Nt}\right)^{\frac{1}{\alpha}} - 1\right]\\ &\simeq \frac{N}{\alpha-1}\left(\frac{P_k}{Nt}\right)^{\frac{1}{\alpha}}.\end{aligned} \tag{42}$$

This completes the proof. □

In addition, for the case that $|\chi_1\rangle$ is a product state, $t \ll N$ and $\alpha = \frac{1}{2}$ in equation (34), the skew information of coherence of the state $|\psi_{kH_O}\rangle$ is given by

$$C_s(\rho_{kH_O}) \simeq 1 - \frac{P_k^2}{t^2N}. \tag{43}$$

Taking the limit $\alpha \to 1$ in equation (40), the relative entropy of coherence of the state $|\psi_{kH_O}\rangle$ is given by

$$\begin{aligned}C_r(\rho_{kH_O}) &\simeq -\frac{P_kt}{N\ln 2}\ln\frac{P_kt}{N} - \frac{P_k}{t\ln 2}\ln\frac{P_k}{Nt}\\ &\simeq \frac{P_k}{t\ln 2}\ln\frac{Nt}{P_k}.\end{aligned} \tag{44}$$

We now explore the coherence of the state $|\psi_{kH_O}\rangle$ when the number of the target states is small ($t \leqslant 4$).

• When $t = 1$, the database has one single target state, $|\chi_1\rangle$ is always a product state. According to Theorem 3 we get

$$C_\alpha(\rho_{kH_O}) \simeq \frac{1}{\alpha-1}[P_k^{\frac{1}{\alpha}}N^{1-\frac{1}{\alpha}} - 1], \tag{45}$$

when $\alpha \in (0, 1)$, and

$$C_\alpha(\rho_{kH_O}) \simeq \frac{N}{\alpha-1}\left(\frac{P_k}{N}\right)^{\frac{1}{\alpha}}, \tag{46}$$

when $\alpha \in (1, 2]$.

• When $t = 2$, we denote the two target states by $|x_{11}\rangle$ and $|x_{12}\rangle$, respectively. We have $|t - 2t_y| = 1$ for either $|x_{11}\rangle = 0$ or $|x_{11}\rangle \neq 0$ [69]. Thus $\gamma(t, t_y) = \frac{1}{2}$.

(1) When $\alpha \in (0,1)$, according to equation (23) we have

$$C_\alpha(\rho_{kH_O}) \simeq \frac{1}{\alpha-1}\left[\left(\frac{P_k}{2}\right)^{\frac{1}{\alpha}}N^{1-\frac{1}{\alpha}} - 1\right]. \tag{47}$$

(2) When $\alpha \in (1, 2]$, according to equation (25) we obtain

$$C_\alpha(\rho_{kH_O}) \simeq \frac{N}{\alpha-1}\left(\frac{P_k}{2N}\right)^{\frac{1}{\alpha}}. \tag{48}$$

• When $t = 3$, $|t - 2t_y| = \frac{3}{2}$ and $\gamma(t, t_y) = \frac{3}{4}$.

(1) According to equation (23) we get

$$C_\alpha(\rho_{kH_O}) \simeq \frac{1}{\alpha-1}\left[\left(\frac{3P_k}{4}\right)^{\frac{1}{\alpha}}N^{1-\frac{1}{\alpha}} - 1\right], \tag{49}$$

for $\alpha \in (0, 1)$,

(2) for $\alpha \in (1, 2]$,

$$C_\alpha(\rho_{kH_O}) \simeq \frac{N}{\alpha - 1}\left(\frac{3P_k}{4N}\right)^{\frac{1}{\alpha}}. \tag{50}$$

• When $t = 4$, there are two cases that $|\chi_1\rangle$ is either a product state or not.

Case 1: $|\chi_1\rangle$ is a product state. It is observed that $|t - 2t_y| = 1$ [69] and $\gamma(t, t_y) = \frac{1}{4}$.

(1) When $\alpha \in (0, 1)$ we obtain

$$C_\alpha(\rho_{kH_O}) \simeq \frac{1}{\alpha - 1}\left[\left(\frac{P_k}{4}\right)^{\frac{1}{\alpha}} N^{1-\frac{1}{\alpha}} - 1\right]. \tag{51}$$

(2) When $\alpha \in (1, 2]$ the coherence of the state $|\psi_{kH_O}\rangle$ is

$$C_\alpha(\rho_{kH_O}) \simeq \frac{N}{\alpha - 1}\left(\frac{P_k}{4N}\right)^{\frac{1}{\alpha}}. \tag{52}$$

Case 2: $|\chi_1\rangle$ is not a product state. It is observed that $|t - 2t_y| = \frac{3}{2}$ [69] and $\gamma(t, t_y) = \frac{9}{16}$.

(1) When $\alpha \in (0, 1)$ we have

$$C_\alpha(\rho_{kH_O}) \simeq \frac{1}{\alpha - 1}\left[\left(\frac{9P_k}{16}\right)^{\frac{1}{\alpha}} N^{1-\frac{1}{\alpha}} - 1\right]. \tag{53}$$

(2) When $\alpha \in (1, 2]$, the coherence of the state $|\psi_{kH_O}\rangle$ is

$$C_\alpha(\rho_{kH_O}) \simeq \frac{N}{\alpha - 1}\left(\frac{9P_k}{16N}\right)^{\frac{1}{\alpha}}. \tag{54}$$

**Remark 4.1.** (1) When $t$=1 and $\alpha = \frac{1}{2}$ in equation (45), according to equation (44) the skew information of coherence and the relative entropy of coherence of the state $|\psi_{kH_O}\rangle$ are

$$C_s(\rho_{kH_O}) \simeq 1 - \frac{P_k^2}{N} \text{ and } C_r(\rho_{kH_O}) \simeq \frac{P_k}{\ln 2} \ln \frac{N}{P_k},$$

respectively.

(2) When $t$=2, $\alpha = \frac{1}{2}$ in equation (47), according to equation (33) the skew information of coherence and the relative entropy of coherence of the state $|\psi_{kH_O}\rangle$ are

$$C_s(\rho_{kH_O}) \simeq 1 - \frac{P_k^2}{4N} \text{ and } C_r(\rho_{kH_O}) \simeq \frac{P_k}{2\ln 2} \ln \frac{2N}{P_k},$$

respectively.

(3) When $t = 3$ and $\alpha = \frac{1}{2}$ in equation. (49), according to equation (33) the skew information of coherence and the relative entropy of coherence of the state $|\psi_{kH_O}\rangle$ are

$$C_s(\rho_{kH_O}) \simeq 1 - \frac{9P_k^2}{16N} \text{ and } C_r(\rho_{kH_O}) \simeq \frac{3P_k}{4\ln 2} \ln \frac{4N}{3P_k},$$

respectively.

(4) When $t = 4$, there are two cases.

Case 1: Set $\alpha = \frac{1}{2}$ in equation (51). According to equation (33) the skew information of coherence and the relative entropy of coherence of the state $|\psi_{kH_O}\rangle$ are

$$C_s(\rho_{kH_O}) \simeq 1 - \frac{P_k^2}{16N} \text{ and } C_r(\rho_{kH_O}) \simeq \frac{P_k}{4\ln 2} \ln \frac{4N}{P_k},$$

respectively.

Case 2: Set $\alpha = \frac{1}{2}$ in equation (53). According to equation (33), the skew information of coherence and the relative entropy of coherence of the state $|\psi_{kH_O}\rangle$ are

$$C_s(\rho_{kH_O}) \simeq 1 - \frac{81P_k^2}{256N} \text{ and } C_r(\rho_{kH_O}) \simeq \frac{9P_k}{16\ln 2} \ln \frac{16N}{9P_k},$$

respectively.

According to Theorem 3 and equations (51), (52), (53) and (54), when $\alpha \in (1, 2]$ the Tsallis relative $\alpha$ entropy of coherence of the state $|\psi_{kH_O}\rangle$ is larger when the superposition state of the targets is an entangled one. However, when $\alpha \in (0, 1)$ it is found that the coherence is smaller when the superposition state of the targets is entangled.

**Conjecture** The Tsallis relative $\alpha$ entropy of coherence of the state $|\psi_{kH_O}\rangle$ relies on the size of the database $N$, the success probability and the target states.

(1) For $\alpha \in (0,1)$, the coherence of $|\psi_{kH_O}\rangle$ reaches the lower bound when $t$=1, and the coherence of $|\psi_{kH_O}\rangle$ reaches the upper bound when $|\chi_1\rangle$ is a product state. It holds that

$$\frac{1}{\alpha - 1}[P_k^{\frac{1}{\alpha}} N^{1-\frac{1}{\alpha}} - 1] \leqslant C_\alpha(\rho_{kH_O}) \leqslant \frac{1}{\alpha - 1}\left[\left(\frac{P_k}{t}\right)^{\frac{1}{\alpha}} N^{1-\frac{1}{\alpha}} - 1\right].$$

(2) For $\alpha \in (1, 2]$, the coherence of $|\psi_{kH_O}\rangle$ reaches the upper bound when $t = 1$, and the coherence of $|\psi_{kH_O}\rangle$ reaches the lower bound when $|\chi_1\rangle$ is a product state. It holds that

$$\frac{N}{\alpha - 1}\left(\frac{P_k}{Nt}\right)^{\frac{1}{\alpha}} \leqslant C_\alpha(\rho_{kH_O}) \leqslant \frac{N}{\alpha - 1}\left(\frac{P_k}{N}\right)^{\frac{1}{\alpha}}.$$

## 5. Production and depletion of Tsallis relative $\alpha$ entropy of coherence

The coherence of a state changes when the operators $H_P$ and $H_O$ are applied. In this section, we investigate how the coherence changes before and after these operators are applied, i.e. the production and depletion of the Tsallis relative $\alpha$ entropy of coherence for $\alpha \in (1, 2]$. In order to clarify the variations and connections of operator coherence in GSA, we also provide some examples and diagrammatic sketches related to the coherence dynamics.

We first introduce the following definitions. The variations of operator coherence between two consecutive iterations of $H_O$, $H_P$ and $G$ in GSA are defined as

$$\Delta C^\alpha(\rho_{kG}) \equiv C_\alpha^\alpha(\rho_{k+1}) - C_\alpha^\alpha(\rho_k), \tag{55}$$

$$\Delta C^\alpha(\rho_{kH_O}) \equiv C_\alpha^\alpha(\rho_{(k+1)H_O}) - C_\alpha^\alpha(\rho_{kH_O}), \tag{56}$$

$$\Delta C^{\alpha}(\rho_{kH_P}) \equiv C_{\alpha}^{\alpha}(\rho_{(k+1)H_P}) - C_{\alpha}^{\alpha}(\rho_{kH_P}). \quad (57)$$

The variations of suboperator coherence of each basic operator $H_O$ and $H_P$ in one Grover iteration are defined as

$$\Delta C^{\alpha}(\rho_{k\Delta H_O}) \equiv C_{\alpha}^{\alpha}(\rho_{kH_O}) - C_{\alpha}^{\alpha}(\rho_k), \quad (58)$$

$$\Delta C^{\alpha}(\rho_{k\Delta H_P}) \equiv C_{\alpha}^{\alpha}(\rho_{kH_P}) - C_{\alpha}^{\alpha}(\rho_{kH_O}). \quad (59)$$

Concerning the production and depletion of coherence for basic operators in GSA, we have the following conclusion.

**Theorem 4.** For $\alpha \in (1, 2]$ and $t \ll N$, the variations and connections of operator coherence between two consecutive iterations of $H_O$, $H_P$ and $G$ in GSA are given by

$$\begin{aligned}
\Delta C^{\alpha}(\rho_{kG}) &\simeq \frac{N^{\alpha-1}}{(\alpha-1)^{\alpha}}(P_k - P_{k+1}) < 0,\\
\Delta C^{\alpha}(\rho_{kH_O}) &\simeq \frac{N^{\alpha-1}}{(\alpha-1)^{\alpha}}\gamma(t, t_y)(P_{k+1} - P_k) > 0,\\
\Delta C^{\alpha}(\rho_{kH_P}) &\simeq \frac{N^{\alpha-1}}{(\alpha-1)^{\alpha}}(P_{k+1} - P_{k+2}) < 0,
\end{aligned} \quad (60)$$

and

$$\Delta C^{\alpha}(\rho_{kG}) \simeq \Delta C^{\alpha}(\rho_{(k-1)H_P}) \simeq -\frac{1}{\gamma(t, t_y)}\Delta C^{\alpha}(\rho_{kH_O}). \quad (61)$$

*Proof*. Combining equations (8) with (55), it is easy to obtain

$$\Delta C^{\alpha}(\rho_{kG}) \simeq \frac{N^{\alpha-1}}{(\alpha-1)^{\alpha}}(P_k - P_{k+1}).$$

Since $P_k < P_{k+1}$, we have

$$\Delta C^{\alpha}(\rho_{kG}) \simeq \frac{N^{\alpha-1}}{(\alpha-1)^{\alpha}}(P_k - P_{k+1}) < 0.$$

Similarly, according to equations (25) and (56), it is easy to get

$$\Delta C^{\alpha}(\rho_{kH_O}) \simeq \frac{N^{\alpha-1}}{(\alpha-1)^{\alpha}}\gamma(t, t_y)(P_{k+1} - P_k) > 0.$$

Combining equations (26) with (57), we have

$$\Delta C^{\alpha}(\rho_{kH_P}) \simeq \frac{N^{\alpha-1}}{(\alpha-1)^{\alpha}}(P_{k+1} - P_{k+2}) < 0.$$

Obviously, we have the following relationship among these variations,

$$\Delta C^{\alpha}(\rho_{kG}) \simeq \Delta C^{\alpha}(\rho_{(k-1)H_P}) \simeq -\frac{1}{\gamma(t, t_y)}\Delta C^{\alpha}(\rho_{kH_O}).$$

According to Theorem 4, the operator coherence between two consecutive iterations of $H_P$ and $G$ is depleted. Both of them rely on the size of the database $N$ and the success probability. Correspondingly, the operator coherence between two consecutive iterations of $H_O$ is produced, which relies on the size of the database $N$, the success probability and target states.

**Theorem 5.** For $\alpha \in (1,2]$ and $t \ll N$, the functions $\Delta C^{\alpha}(\rho_{kH_P})$ and $\Delta C^{\alpha}(\rho_{kH_O})$ have a turning point. The variations of the suboperator coherence of each basic operator $H_O$ and $H_P$ in one Grover iteration are given by

$$\Delta C^{\alpha}(\rho_{k\Delta H_O}) \simeq \frac{N^{\alpha-1}}{(\alpha-1)^{\alpha}}[(\gamma(t, t_y) + 1)P_k - 1], \quad (62)$$

$$\Delta C^{\alpha}(\rho_{k\Delta H_P}) \simeq \frac{N^{\alpha-1}}{(\alpha-1)^{\alpha}}[1 - (\gamma(t, t_y)P_k + P_{k+1})]. \quad (63)$$

*Proof*. According to equations (8), (25) and (58), we have (62). Similarly, by substituting equations (25) and (26) into (59), we obtain (63). There exists a turning point $k_T$ at which $\Delta C^{\alpha}(\rho_{k\Delta H_O}) = 0$. This is equivalent to $(\gamma(t, t_y) + 1)P_k - 1 = 0$, namely,

$$k_T \simeq \left\lfloor \frac{\arcsin\sqrt{\dfrac{1}{\gamma(t, t_y) + 1}}}{2\theta} \right\rfloor.$$

Similar results can be obtained for $\Delta C^{\alpha}(\rho_{k\Delta H_P}) = 0$. □

According to Theorem 5, for $t \ll N$ we have $\Delta C^{\alpha}(\rho_{k\Delta H_O})<0$ and $\Delta C^{\alpha}(\rho_{k\Delta H_P})>0$ when $(\gamma(t, t_y) + 1)P_k<1$, and $\Delta C^{\alpha}(\rho_{k\Delta H_O})>0$ and $\Delta C^{\alpha}(\rho_{k\Delta H_P})<0$ when $(\gamma(t, t_y) + 1)P_k>1$. The Tsallis relative $\alpha$ entropy of coherence of $H_O$ and $H_P$ show different effects that one depletes coherence and the other produces coherence. Moreover, the operator coherence of $H^{\otimes n}$ is not always produced or depleted, but depleted and produced alternatively. Before the turning point, the operator coherence of $H_O$ is depleting, and the operator coherence of $H_P$ is producing. However, the situation is reversed after the turning point.

We now use examples and plots to illustrate the characters of coherence of the state after each basic operator is applied in GSA, how these operators contribute to coherence, and the relationships among the coherence of the operators and the success probability.

**Example 1** Suppose that the qubit numbers are $n = 16$ and the target numbers are $t = 2$. In this case $\gamma(t, t_y) = \frac{1}{2}$. Based on Theorem 5, the suboperator coherence of $O$ and $P$ in one Grover iteration are unaltered. When $k < k_T$ the suboperator coherence of $H_O$ in one Grover iteration is depleting, and the suboperator coherence of $H_P$ is producing. However, when $k > k_T$ the situation is reversed. Figure 1 shows the variations of the suboperator coherence of each basic operator $O$, $H_O$, $P$ and $H_P$ in one Grover iteration. For clarity in figure 1 we use $\frac{((\alpha-1)C_{\alpha})^{\alpha}}{N^{\alpha-1}}$ as the vertical axis. From figure 1 we see that before the turning point, the suboperator coherence of each basic operator $O$, $H_O$, $P$ and $H_P$ in one Grover iteration are unchanged, decreased, unchanged and increased, respectively; while after the turning point, they are unchanged, increased, unchanged and decreased, respectively.

Figure 2 shows that the success probability $P_k$ increases with the increase of the number of iterations. According to equations (25) and (26), the operator coherence of $H^{\otimes n}$

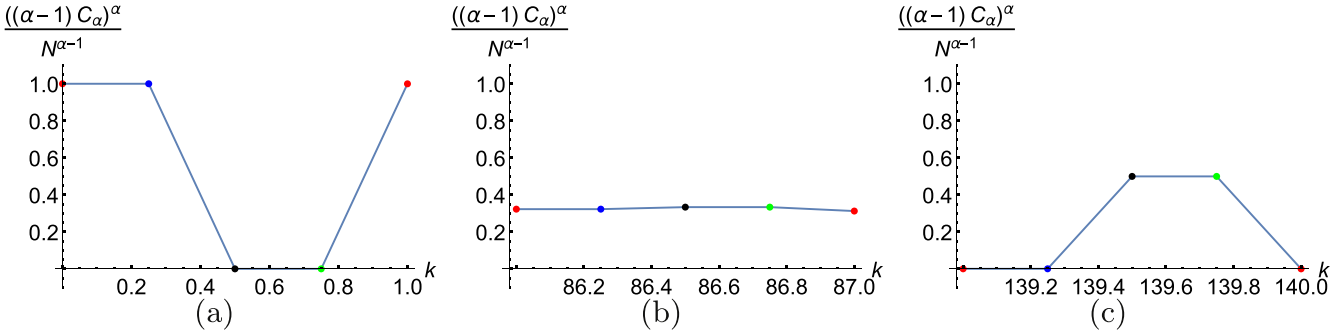


**Figure 1.** The coherence dynamics in one Grover iteration. The red, blue, black and green dots are the coherences of $O$, $H_O$, $P$ and $H_P$, respectively. The variations of the suboperator coherence before the turning point (a), at the turning point (b) and after the turning point (c).

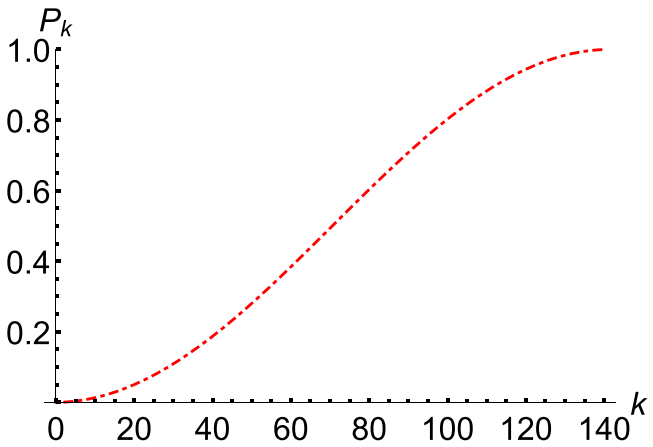


**Figure 2.** The variations of success probability $P_k$ (red dot-dashed line) as a function of the number of iterations $k$.

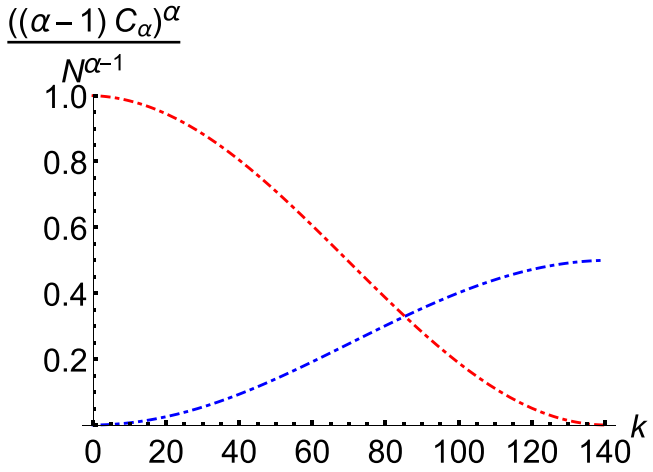


**Figure 3.** The operator coherence of $H^{\otimes n}$. The blue dot-dashed line and red dot-dashed line represent the operator coherence of $H_O$ and $H_P$, respectively.

vibrates between $1 - P_{k+1}$ and $\gamma(t, t_y)P_k$. The relations between the operator coherence of $H^{\otimes n}$ and the operator coherence of $H_O$ and $H_P$ are shown in figure 3. The intersection of the two lines is the turning point.

In figure 4, we illustrate the relationships of $\Delta C^\alpha(\rho_{kG})$, $\Delta C^\alpha(\rho_{kH_P})$ and $\Delta C^\alpha(\rho_{kH_O})$ between two consecutive iterations.

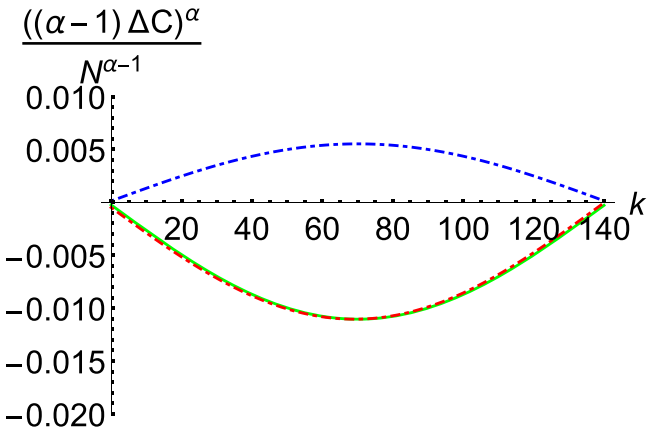


**Figure 4.** The operator coherence of $G$ (green), $H_P$ (red dot-dashed) and $H_O$ (blue dot-dashed) between two consecutive iterations.

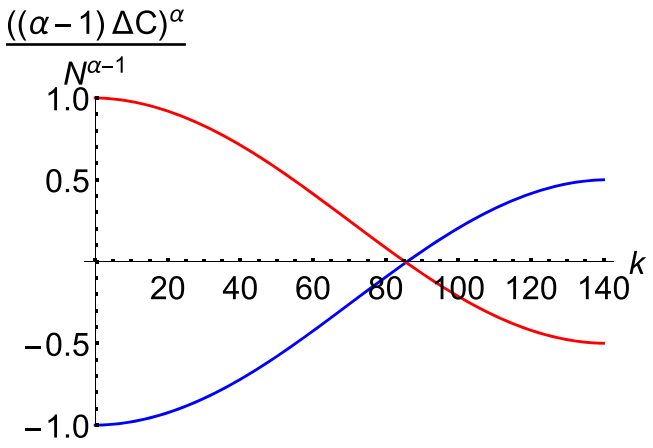


**Figure 5.** The suboperator coherence of $H_P$ (red) and $H_O$ (blue) in one Grover iteration.

According to Theorem 3, we have $\Delta C^\alpha(\rho_{kG}) \simeq \Delta C^\alpha(\rho_{(k-1)H_P}) \simeq -\dfrac{1}{\gamma(t, t_y)}\Delta C^\alpha(\rho_{kH_O})$, which are zero at the beginning and the end. The connections of the suboperator coherence of $H_P$ and $H_O$ in one Grover iteration are shown in figure 5. Moreover, the coherence of $H_P$ ($H_O$) is 1 ($-1$) at the beginning and $-\frac{1}{2}$ $\left(\frac{1}{2}\right)$ at the end.

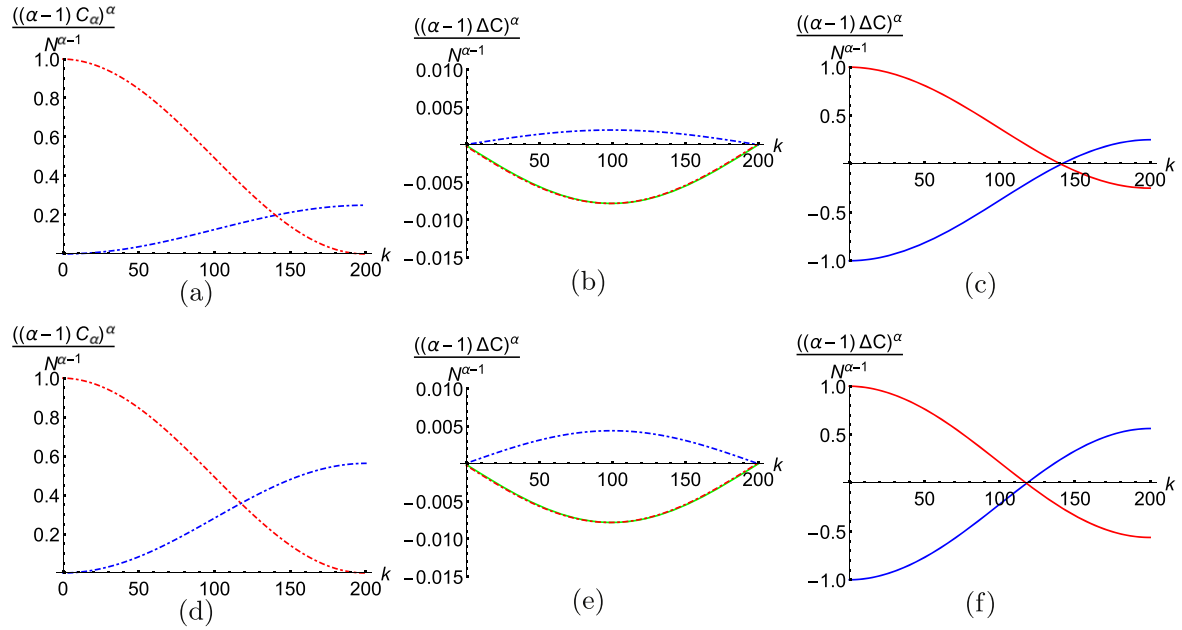


**Figure 6.** Subfigures (a)–(f) are for the case that the superposition state of targets is a product one (an entangled one). (a), (d) The relationships of the operator coherence of $H_P$ and $H_O$. (b), (e) The relationships of $\Delta C^{\alpha}(\rho_{kG})$, $\Delta C^{\alpha}(\rho_{kH_P})$ and $\Delta C^{\alpha}(\rho_{kH_O})$ between two consecutive iterations. (c), (f) The connections of the suboperator coherence of $H_P$ and $H_O$ in one Grover iteration.

**Example 2** Consider that the qubit numbers are $n = 18$ and the target numbers are $t = 4$. In this case $\gamma(t, t_y) = \frac{9}{16}$ when the superposition state of targets is entangled and $\gamma(t, t_y) = \frac{1}{4}$ when superposition state is a product one. From Theorem 3 the Tsallis relative $\alpha$ entropy of coherence of $|\psi_{kH_O}\rangle$ is larger when the superposition state of targets is entangled for $\alpha \in (1, 2]$. When the superposition state of targets is entangled, we show in figure 6 the relationships between the operator coherence of $H_P$ and $H_O$, the relationships among $\Delta C^{\alpha}(\rho_{kG})$, $\Delta C^{\alpha}(\rho_{kH_P})$ and $\Delta C^{\alpha}(\rho_{kH_O})$ between two consecutive iterations, and the connections between the suboperator coherence of $H_P$ and $H_O$ in one Grover iteration. For comparison, we also present the corresponding results when the superposition state of targets is a product one.

Note that Tsallis relative $\alpha$ entropy of coherence incorporates two important coherence quantifiers, the relative entropy of coherence and the skew information of coherence, so using such technical methods of Tsallis relative $\alpha$ entropy to study coherent dynamics may yield more information about the properties of different coherent measures in GSA. It can also be seen from the examples that entanglement has an important contribution to operator coherence in GSA.

## 6. Comparison with previous works

In order to clarify the contribution of this paper, we compare our work with previous related works in this section.

In [69], the authors have investigated the $l_1$ norm of coherence of the states after each of $O$, $P$ and $H^{\otimes n}$ is applied in one $G$ iteration, and discussed the number of coherence for different cases of the target states. It is shown that the coherence is monotone decreasing with the increase of the success probability, and it is proved that the coherence is vibrating, the overall effect is that coherence is in depletion. Moreover, the coherence is larger when the superposition state of targets is an entangled one.

In this work, we study coherence dynamics in GSA based on Tsallis relative $\alpha$ entropy. The amount of coherence of first $H^{\otimes n}$ depends on the size of the database $N$, success probability and target states, and the coherence of two $H^{\otimes n}$ have different effects that one depletes coherence and the other produces coherence. Coherence is not always produced or depleted, but depleted and produced in turn. When $\alpha \in (0,1)$, the coherence is smaller when the superposition state of targets is an entangled one, and the coherence reduction is not monotonic, but related to the parameter $\alpha$ with the increase of the success probability, which is different from [69].

On the other hand, in [47], the Grover iteration has been decomposed into two basic operators $R$ and $O$, where $R = H^{\otimes n}PH^{\otimes n}$. It is demonstrated that $H^{\otimes n}$ does not change entanglement, and there exists a turning point during the application of the algorithm. Before the turning point, the entanglement always increases when the operator $O$ is applied, and the effect of the operator $R$ can be almost ignored on the level of entanglement. After the turning point, the $R$ remarkably decreases entanglement, and $O$ increases entanglement. In our work, we study the coherence of the states on the essential operator level and show that operators $O$ and $P$ do not change the coherence. In addition, we also obtain a turning point when $\alpha \in (1,2]$. Before the turning point, the operator coherence of $H_O$ is depleting, and the operator coherence of $H_P$ is producing. After the turning point, the situation is reversed.

## 7. Conclusions and discussions

We have explored the coherence dynamics in GSA based on Tsallis relative $\alpha$ entropy for $\alpha \in (0, 1) \cup (1, 2]$, and proved that the coherence decreases with the increase of the success probability. We have derived the complementarity relations between Tsallis relative $\alpha$ entropy of coherence and the success probability. Moreover, we have studied how each basic operator contributes to the coherence in GSA, and proved that the amount of operator coherence of $H_O$ relies on the size of the database $N$, the success probability and the target states. Following the idea in [69], we have also discussed the operator coherence of $|\psi_{kH_O}\rangle$ for different target states. Finally, when $\alpha \in (1, 2]$, we have derived the variations of operator coherence between two consecutive iterations of $H_O$, $H_P$ and $G$ in GSA, and the variations of suboperator coherence of each basic operator $H_O$ and $H_P$ in one Grover iteration. The operators $H_O$ and $H_P$ have different effects on coherence, one produces coherence and another depletes it. Coherence of the $H^{\otimes n}$ is not always depleted but depleted and produced alternatively. It oscillates during GSA application.

In addition, when $\alpha \in (0, 1)$ and $\alpha \in (1, 2]$, the entangled target state has different impacts on the Tsallis relative $\alpha$ entropy of coherence. When $\alpha \in (0, 1)$, the coherence is smaller when the superposition state of targets is an entangled one. However, when $\alpha \in (1, 2]$, the coherence is larger when the superposition state of targets is an entangled one. It would be interesting to study how the entanglement of the superposition state of targets is related to the coherence quantitatively. Our results may shed some new light on the study of the coherence dynamics in quantum algorithms, and provide new insights into quantum information processing tasks.

Utilizing the relative entropy of coherence and the $l_1$ norm of coherence, it has been pointed out in [70] that coherence of the system states reduces to the minimum in company with the successful implementation of Grover's algorithm. In this paper, we can draw the same conclusion when the Tsallis relative $\alpha$ entropy of coherence is employed. Nevertheless, a similar assertion does not hold if other quantifiers of a resource, like quantum entanglement, are used. This peculiar character of quantum coherence may be beneficial for designing new quantum algorithms in the future.

## Acknowledgments

The authors would like to express their sincere gratitude to the anonymous referees, which greatly improved this paper. This work was supported by the National Natural Science Foundation of China (Grant Nos. 12161056, 12075159, 12171044); Beijing Natural Science Foundation (Grant No. Z190005); the Academician Innovation Platform of Hainan Province.

## Competing interests

The authors declare no competing interests.

## References

[1] Baumgratz T, Cramer M and Plenio M B 2014 Quantifying coherence *Phys. Rev. Lett.* **113** 140401
[2] Winter A and Yang D 2016 Operational resource theory of coherence *Phys. Rev. Lett.* **116** 120404
[3] Chitambar E and Gour G 2019 Quantum resource theories *Rev. Mod. Phys.* **91** 025001
[4] Rana S, Parashar P and Lewenstein M 2016 Trace-distance measure of coherence *Phys. Rev.* A **93** 012110
[5] Piani M, Cianciaruso M, Bromley T R, Napoli C, Johnston N and Adesso G 2016 Robustness of asymmetry and coherence of quantum states *Phys. Rev.* A **93** 042107
[6] Yu C-S 2017 Quantum coherence via skew information and its polygamy *Phys. Rev.* A **95** 042337
[7] Wu Z, Zhang L, Fei S-M and Li-Jost X 2020 Coherence and complementarity based on modified generalized skew information *Quantum Inf. Process.* **19** 1–20
[8] Yu X, Zhang D, Xu G and Tong D 2016 Alternative framework for quantifying coherence *Phys. Rev.* A **94** 060302
[9] Zhu X-N, Jin Z-X and Fei S-M 2019 Quantifying quantum coherence based on the generalized $\alpha$-z-relative Rényi entropy *Quantum Inf. Process.* **18** 179
[10] Xiong C, Kumar A and Wu J 2018 Family of coherence measures and duality between quantum coherence and path distinguishability *Phys. Rev.* A **98** 032324
[11] Chitambar E and Hsieh M-H 2016 Relating the resource theories of entanglement and quantum coherence *Phys. Rev. Lett.* **117** 020402
[12] Ma J, Yadin B, Girolami D, Vedral V and Gu M 2016 Converting coherence to quantum correlations *Phys. Rev. Lett.* **116** 160407
[13] Xi Z, Li Y and Fan H 2015 Quantum coherence and correlations in quantum system *Sci. Rep.* **5** 10922
[14] Yao Y, Xiao X, Ge L and Sun C 2015 Quantum coherence in multipartite systems *Phys. Rev.* A **92** 022112
[15] Qi X, Gao T and Yan F 2017 Measuring coherence with entanglement concurrence *J. Phys. A: Math. Theor.* **50** 285301
[16] Du S, Bai S and Qi X 2015 Coherence measures and optimal conversion for coherent states *Quantum Inf. Comput.* **15** 1307
[17] Du S, Bai Z and Guo Y 2015 Conditions for coherence transformations under incoherent operations *Phys. Rev.* A **91** 052120
[18] Bromley T R, Cianciaruso M and Adesso G 2015 Frozen quantum coherence *Phys. Rev. Lett.* **114** 210401
[19] Wang J, Tian Z, Jing J and Fan H 2016 Irreversible degradation of quantum coherence under relativistic motion *Phys. Rev.* A **93** 062105
[20] Yu X, Zhang D, Liu C and Tong D 2016 Measure-independent freezing of quantum coherence *Phys. Rev.* A **93** 060303
[21] Peng Y, Jiang Y and Fan H 2016 Maximally coherent states and coherence-preserving operations *Phys. Rev.* A **93** 032326
[22] Mani A and Karimipour V 2015 Cohering and decohering power of quantum channels *Phys. Rev.* A **92** 032331
[23] Radhakrishnan C, Parthasarathy M, Jambulingam S and Byrnes T 2016 Distribution of quantum coherence in multipartite systems *Phys. Rev. Lett.* **116** 150504

[24] Wu Z, Huang H, Fei S-M and Li-Jost X 2020 Geometry of skew information-based quantum coherence *Commun. Theor. Phys.* **72** 105102

[25] Huang H, Wu Z and Fei S-M 2021 Uncertainty and complementarity relations based on generalized skew information *Europhys. Lett.* **132** 60007

[26] Wu Z, Zhang L, Fei S-M and Li-Jost X 2021 Average skew information-based coherence and its typicality for random quantum states *J. Phys. A: Math. Theor.* **54** 015302

[27] Wu Z, Zhang L, Fei S-M and Wang J 2022 Skew information-based coherence generating power of quantum channels *Quantum Inf. Process.* **21** 236

[28] Xu J 2016 Quantifying coherence of Gaussian states *Phys. Rev.* A **93** 032111

[29] Zhang Y, Shao L, Li Y and Fan H 2016 Quantifying coherence in infinite-dimensional systems *Phys. Rev.* A **93** 012334

[30] Huelga S F and Plenio M B 2013 Vibrations, quanta and biology *Contemp. Phys.* **54** 181

[31] Lloyd S 2011 Quantum coherence in biological systems *J. Phys. Conf. Ser.* **302** 012037

[32] Lostaglio M, Jennings D and Rudolph T 2015 Description of quantum coherence in thermodynamic processes requires constraints beyond free energy *Nat. Commun.* **6** 6383

[33] Lostaglio M, Korzekwa K, Jennings D and Rudolph T 2015 Quantum coherence, time-translation symmetry, and thermodynamics *Phys. Rev.* X **5** 021001

[34] Narasimhachar V and Gour G 2015 Low-temperature thermodynamics with quantum coherence *Nat. Commun.* **6** 7689

[35] Horodecki M and Oppenheim J 2013 Fundamental limitations for quantum and nanoscale thermodynamics *Nat. Commun.* **4** 2059

[36] Kammerlander P and Anders J 2016 Coherence and measurement in quantum thermodynamics *Sci. Rep.* **6** 22174

[37] Karlström O, Linke H, Karlström G and Wacker A 2011 Increasing thermoelectric performance using coherent transport *Phys. Rev.* B **84** 113415

[38] Chen J, Cui J, Zhang Y and Fan H 2016 Coherence susceptibility as a probe of quantum phase transitions *Phys. Rev.* A **94** 022112

[39] Shor P W 1997 Polynomial-time algorithms for prime factorization and discrete logarithms on a quantum computer *SIAM J. Comput.* **26** 1484

[40] Knill E and Laflamme R 1998 Power of one bit of quantum information *Phys. Rev. Lett.* **81** 5672

[41] Simon D R 1997 On the power of quantum computation *SIAM J. Comput.* **26** 1474

[42] Harrow A W, Hassidim A and Lloyd S 2009 Quantum algorithm for linear systems of equations *Phys. Rev. Lett.* **103** 150502

[43] Grover L K 1997 Quantum mechanics helps in searching for a needle in a haystack *Phys. Rev. Lett.* **79** 325

[44] Rungta P 2009 The quadratic speedup in Grover's search algorithm from the entanglement perspective *Phys. Lett.* A **373** 2652

[45] Rossi M, BruÃŸ D and Macchiavello C 2013 Scale invariance of entanglement dynamics in Grover's quantum search algorithm *Phys. Rev.* A **87** 022331

[46] Fang Y, Kaszlikowski D, Chin C, Tay K, Kwek L C and Oh C H 2005 Entanglement in the Grover search algorithm *Phys. Lett.* A **345** 265

[47] Pan M, Qiu D, Mateus P and Gruska J 2019 Entangling and disentangling in Grover's search algorithm *Theor. Comput. Sci.* **773** 138

[48] Tsallis C 1988 Possible generalization of Boltzmann–Gibbs statistics *J. Stat. Phys.* **52** 479

[49] Borland L, Plastino A R and Tsallis C 1998 Information gain within nonextensive thermostatistics *J. Math. Phys.* **39** 6490

[50] Shiino M 1998 H-theorem with generalized relative entropies and the Tsallis statistics *J. Phys. Soc. Jpn.* **67** 3658–60

[51] Tsallis C 1998 Generalized entropy-based criterion for consistent testing *Phys. Rev.* E **58** 1442

[52] Abe S 2003 Nonadditive generalization of the quantum Kullback–Leibler divergence for measuring the degree of purification *Phys. Rev.* A **68** 032302

[53] Abe S 2003 Monotonic decrease of the quantum nonadditive divergence by projective measurements *Phys. Rev.* A **312** 336

[54] Furuichi S, Yanagi K and Kuriyama K 2004 Fundamental properties of Tsallis relative entropy *J. Math. Phys.* **45** 4868

[55] Rastegin A E 2016 Quantum-coherence quantifiers based on the Tsallis relative $\alpha$ entropies *Phys. Rev.* A **93** 032136

[56] Zhao H and Yu C 2018 Coherence measure in terms of the Tsallis relative $\alpha$ entropy *Sci. Rep.* **8** 299

[57] Streltsov A, Singh U, Dhar H S, Bera M N and Adesso G 2015 Measuring quantum coherence with entanglement *Phys. Rev. Lett.* **115** 020403

[58] Zhang F, Shao L, Luo Y and Li Y 2017 Ordering states with Tsallis relative $\alpha$-entropies of coherence *Quantum Inf. Process.* **16** 31

[59] Bu K, Garcia R J, Jaffe A, Koh D E and Li L 2022 Complexity of quantum circuits via sensitivity, magic, and coherence arXiv:2204.12051

[60] Rall P 2021 Faster coherent quantum algorithms for phase, energy, and amplitude estimation *Quantum* **5** 566

[61] Berberich J, Fink D and Holm C 2023 Robustness of quantum algorithms against coherent control errors arXiv:2303.00618

[62] Koch D, Torrance A, Kinghorn D, Patel S, Wessing L and Alsing P M 2019 Simulating quantum algorithms using fidelity and coherence time as principle models for error arXiv:1908.04229

[63] Escalera-Moreno L 2023 QBithm: towards the coherent control of robust spin qubits in quantum algorithms arXiv:2303.12655

[64] Mahdian M and Yeganeh H D 2020 Incoherent quantum algorithm dynamics of an open system with near-term devices *Quantum Inf. Process.* **19** 285

[65] Cirstoiu C, Holmes Z, Iosue J, Cincio L, Coles P J and Sornborger A 2020 Variational fast forwarding for quantum simulation beyond the coherence time *NPJ Quantum Inf.* **6** 82

[66] Berthusen N F, Trevisan T V, Iadecola T and Orth P P 2022 Quantum dynamics simulations beyond the coherence time on noisy intermediate-scale quantum hardware by variational trotter compression *Phys. Rev. Res.* **4** 023097

[67] Hillery M 2016 Coherence as a resource in decision problems: The Deutsch–Jozsa algorithm and a variation *Phys. Rev.* A **93** 012111

[68] Matera J M, Egloff D, Killoran N and Plenio M B 2016 Coherent control of quantum systems as a resource theory *Quantum Sci. Technol.* **1** 01LT01

[69] Pan M and Qiu D 2019 Operator coherence dynamics in Grover's quantum search algorithm *Phys. Rev.* A **100** 012349

[70] Liu Y, Shang J and Zhang X 2019 Coherence depletion in quantum algorithms *Entropy* **21** 260

[71] Shi H, Liu S, Wang X, Yang W-L, Yang Z-Y and Fan H 2017 Coherence depletion in the Grover quantum search algorithm *Phys. Rev.* A **95** 032307

[72] Pan M, Situ H and Zheng S 2022 Complementarity between success probability and coherence in Grover search algorithm *Europhys. Lett.* **138** 48002

[73] Ahnefeld F, Theurer T, Egloff D, Matera J M and Plenio M B 2022 Coherence as a resource for Shor's algorithm *Phys. Rev. Lett.* **129** 120501

[74] Bettelli S and Shepelyansky D L 2003 Entanglement versus relaxation and decoherence in a quantum algorithm for quantum chaos *Phys. Rev.* A **67** 054303
[75] Hong C, Heo J, Kang M, Jang J, Yang H and Kwon D 2019 Photonic scheme of quantum phase estimation for quantum algorithms via cross-Kerr nonlinearities under decoherence effect *Opt. Express* **27** 31023
[76] Song X, Zhang H, Ai Q, Qiu J and Deng F 2016 Shortcuts to adiabatic holonomic quantum computation in decoherence-free subspace with transitionless quantum driving algorithm *New J. Phys.* **18** 023001
[77] Tiersch M and Schützhold R 2007 Non-Markovian decoherence in the adiabatic quantum search algorithm *Phys. Rev.* A **75** 062313
[78] Smith K N, Ravi G S, Murali P, Baker J M, Earnest N, Javadi-Cabhari A and Chong F 2022 TimeStitch: Exploiting slack to mitigate decoherence in quantum circuits *ACM Trans. Quantum Comput.* **4** 1
[79] Naseri M, Kondra T V, Goswami S, Fellous-Asiani M and Streltsov A 2022 Entanglement and coherence in the Bernstein–Vazirani algorithm *Phys. Rev.* A **106** 062429
[80] Anand N and Pati A K 2016 Coherence and entanglement monogamy in the discrete analogue of analog Grover search arXiv:1611.04542
[81] Filgueiras C, Rojas O and Rojas M 2020 Thermal entanglement and correlated coherence in two coupled double quantum dots systems *Ann. Phys.* **532** 2000207
[82] Fu S, He J, Li X and Luo S 2023 Uncertainties and coherence in DQC1 *Phys. Scr.* **98** 045114
[83] Ma J, Yadin B, Girolami D, Vedral V and Gu M 2016 Converting coherence to quantum correlations *Phys. Rev. Lett.* **116** 160407
[84] Wang W *et al* 2019 Witnessing quantum resource conversion within deterministic quantum computation using one pure superconducting qubit *Phys. Rev. Lett.* **123** 220501
[85] Goettems E I, Maciel T O, Soares-Pinto D O and Duzzioni E I 2021 Promoting quantum correlations in deterministic quantum computation with a one-qubit model via postselection *Phys. Rev.* A **103** 042416
[86] Karimi M, Javadi-Abhari A, Simon C and Ghobadi R 2022 The power of one clean qubit in supervised machine learning arXiv:2210.09275
[87] Egloff D, Matera J M, Theurer T and Plenio M B 2018 Of local operations and physical wires *Phys. Rev.* X **8** 031005